

The Aspherical Properties of the Energetic Type Ic SN 2002ap as Inferred from its Nebular Spectra¹

P. A. Mazzali^{2,3,4,5}, K. S. Kawabata⁶, K. Maeda^{2,7}, R. J. Foley⁸, K. Nomoto^{4,5}, J. Deng⁹, T. Suzuki⁴, M. Iye^{10,11}, N. Kashikawa¹⁰, Y. Ohyama¹², A. V. Filippenko⁸, Y. Qiu⁹, and J. Wei⁹

ABSTRACT

The nebular spectra of the broad-lined, SN 1998bw-like Type Ic SN 2002ap are studied by means of synthetic spectra. Two different modelling techniques are employed. In one technique, the SN ejecta are treated as a single zone, while in the other a density and abundance distribution in velocity is used from an explosion model. In both cases, heating caused by γ -ray and positron deposition is computed (in the latter case using a Monte Carlo technique to describe the propagation of γ -rays and positrons), as is cooling via forbidden-line emission. The results are compared, and although general agreement is found, the stratified

¹Based in part on data obtained at the Subaru Telescope, which is operated by the National Astronomical Observatory of Japan (NAOJ). Also based in part on data obtained at the University of California's Lick Observatory.

²Max-Planck Institut für Astrophysik, Karl-Schwarzschild-Str. 1, 85748 Garching, Germany.

³National Institute for Astrophysics–OATs, Via G.B. Tiepolo, 11, 34143 Trieste, Italy.

⁴Department of Astronomy, School of Science, University of Tokyo, Bunkyo-ku, Tokyo 113-0033, Japan.

⁵Research Center for the Early Universe, School of Science, University of Tokyo, Bunkyo-ku, Tokyo 113-0033, Japan.

⁶Hiroshima Astrophysical Science Center, Hiroshima University, Hiroshima 739-8526, Japan.

⁷Department of Earth Science and Astronomy, College of Arts and Sciences, University of Tokyo, Meguro-ku, Tokyo 153-8902, Japan.

⁸Department of Astronomy, University of California, Berkeley, CA 94720-3411.

⁹National Astronomical Observatories, CAS, 20A Datun Road, Chaoyang District, Beijing 100012, China.

¹⁰National Astronomical Observatory of Japan, Mitaka, Tokyo 181-8588, Japan.

¹¹Department of Astronomical Science, Graduate University for Advanced Studies, Mitaka, Tokyo 181-8588, Japan.

¹²Subaru Telescope, National Astronomical Observatory of Japan, 650 North A'ohoku Place, Hilo, HW 96720.

models are shown to reproduce the observed line profiles much more accurately than the single-zone model. The explosion produced $\sim 0.1 M_{\odot}$ of ^{56}Ni . The distribution in velocity of the various elements is in agreement with that obtained from the early-time models, which indicated an ejected mass of $\sim 2.5 M_{\odot}$ with a kinetic energy of 4×10^{51} erg. Nebular spectroscopy confirms that most of the ejected mass ($\sim 1.2 M_{\odot}$) was oxygen. The presence of an oxygen-rich inner core, combined with that of ^{56}Ni at high velocities as deduced from early-time models, suggests that the explosion was asymmetric, especially in the inner part.

Subject headings: supernovae: general —supernovae: individual (SN 2002ap) — nucleosynthesis — gamma rays: bursts

1. Introduction

One of the most exciting recent discoveries in astrophysics is that the nearest observed long-duration gamma-ray bursts (GRBs) are associated with supernovae (SNe) (e.g., GRB980425/SN 1998bw, Galama et al. 1998; GRB030329/SN 2003dh, Stanek et al. 2003; GRB031203/SN 2003lw, Malesani et al. 2004). Adding to the excitement, it turned out that these SNe are not at all ordinary. Spectroscopically, they are of Type Ic (no H, no He, weak Si lines; see Filippenko 1997 for a review of SN classification), but their distinguishing feature is that unlike normal SNe Ic, they show extremely broad absorption lines dominated by Fe, Ca, and O. Very high expansion velocities, reaching $0.1c$, are easily observed at early times.

Broad lines suggest a very energetic explosion, or at least a large amount of energy per unit mass. Estimates of the explosion kinetic energy assuming spherical symmetry for SNe 1998bw, 2003dh, and 2003lw are $E_{\text{kin}} \approx (3 - 6) \times 10^{52}$ erg (e.g., Iwamoto et al. 1998; Nakamura et al. 2001; Mazzali et al. 2003; Deng et al. 2004; Mazzali et al. 2006). This is more than one order of magnitude larger than in typical core-collapse SNe, which have $E_{\text{kin}} \approx 10^{51}$ erg. Accordingly, these exceptionally powerful SNe have sometimes been called “hypernovae” (e.g., Nomoto et al. 2005). In the presence of significant deviations from spherical symmetry, these estimates may be reduced, but even then the energies remain large (e.g., Maeda et al. 2006). The mechanism behind these events is thought to be the collapse of the stripped core of a massive star ($\sim 25 - 60 M_{\odot}$) to a black hole (MacFadyen & Woosley 1999).

Additionally, evidence has been obtained that X-ray flashes (XRFs), the soft analogues of GRBs (Heise et al. 2001), are also linked to SNe (e.g., Fynbo et al. 2003; Modjaz et al. 2006; Pian et al. 2006). The SNe associated with XRFs also seem to be overenergetic,

but not as much so as GRB-SNe (Tominaga et al. 2003; Mazzali et al. 2006). They have been suggested to be the result of the collapse of the stripped carbon-oxygen core of stars of originally $\sim 20 M_{\odot}$ to a neutron star (Mazzali et al. 2006; Maeda et al. 2007). If the neutron star is born highly magnetized and rapidly spinning — a “magnetar” (Duncan & Thompson 1992; Thompson, Chang, & Quataert 2004) — it may cause the explosion to be overenergetic and produce the XRF (Mazzali et al. 2006; Maeda et al. 2007).

One difference between SNe in GRBs and XRFs may be the degree of asphericity. GRB-SNe are thought to be highly aspherical, as GRBs are generally believed to be highly asymmetric phenomena (see Woosley & Bloom 2006 for a recent review of the SN-GRB connection). For XRF-SNe, the degree of asphericity may be smaller (Mazzali et al. 2007).

Evidence for asphericity is not easy to glean from early-time data. The significant mixing outward of ^{56}Ni required to reproduce the early rise of the light curve is a general feature of hypernovae (Maeda et al. 2003) and suggests an aspherical explosion, as does the connection of these SNe with GRBs. The best time to look for signatures of asphericity, however, is starting a few months after the explosion, when the SN becomes nebular, exposing the deepest parts of the ejecta. In that phase, both the spectrum and the light curve have a characteristic behavior. The light curve of SN 1998bw showed a phase of strictly exponential decline, but at a rate steeper than that of ^{56}Co (Patat et al. 2001). In this phase the luminosity is larger than what is predicted by spherically symmetric models that fit the peak of the light curve (Nakamura et al. 2001). Maeda et al. (2003) showed that this behavior, which is actually not unusual in SNe Ic, can be explained using a modified spherically symmetric model where a relatively massive but slowly expanding inner core is placed in the center of the expanding ejecta. Although this is technically still a spherically symmetric model, one-dimensional explosion simulations do not predict such a density distribution, which suggests that we are observing an aspherical explosion, similar perhaps to the collapsar model of MacFadyen & Woosley (1999).

The nebular spectra provide more direct evidence. In SN 1998bw the [Fe II] lines are broader than the [O I] $\lambda\lambda 6300, 6363$ doublet (Mazzali et al. 2001). This is also something that cannot be explained in the context of a spherically symmetric model of the collapse and explosion of a CO core, as in such a model ^{56}Ni (which decays into ^{56}Co and then into ^{56}Fe) is synthesized near the compact remnant and therefore is always located at smaller velocities than O, which is left from the progenitor in the unprocessed outer layers. Maeda et al. (2002) showed that this configuration can be obtained in an axisymmetric explosion. In such an explosion, most of the E_{kin} is released along the “jet” axis, which is probably linked to the launching of the GRB, and ^{56}Ni is synthesized along that direction and ejected at a high velocity. Away from the jet axis, however, less kinetic energy is deposited and burning

proceeds much less efficiently. Therefore, in these directions large amounts of unburned O are ejected at low velocity. For a near-polar viewing angle, this scenario naturally leads to broad [Fe II] lines and a narrow [O I] line at late times. For an equatorial view, on the other hand, the [O I] line should have a characteristic double-peaked profile (Maeda et al. 2002), as was indeed observed in the SN Ic 2003jd (Mazzali et al. 2005). Further evidence that SNe Ic are aspherical also comes from their high degree of polarization (Wang et al. 2001; Leonard et al. 2002; Filippenko & Leonard 2004; Leonard & Filippenko 2005).

For XRF/SNe, the case for asphericity is much weaker. The early-time spectra of SN 2006aj did not show very broad features (Pian et al. 2006). Radio observations (Soderberg et al. 2006) suggest a very broad opening angle ($> 60^\circ$). The broad nebular lines are not inconsistent with spherically symmetric ejecta (Mazzali et al. 2007). Nevertheless, the presence of emission at velocities below 2000 km s^{-1} is at odds with the prediction of one-dimensional explosion models, that a density hole is present at the lowest velocities (Mazzali et al. 2007; Maeda et al. 2007).

Besides those clearly associated with GRBs or XRFs, other energetic SNe Ic have been observed. Energetic SNe Ic, with or without a GRB, are recognized from the extreme width (up to $\sim 0.1c$) of their spectral lines at early times, and have sometimes also been called hypernovae (although their total energy is not always much higher than that of normal SNe Ic). The nearest such object ever observed was SN 2002ap in M74. SN 2002ap was immediately recognized as a broad-lined event, similar spectroscopically to SN 1998bw (Kinugasa et al. 2002), and was therefore intensively observed. SN 2002ap remained much less luminous than SN 1998bw (Mazzali et al. 2002; Gal-Yam, Ofek, & Shemmer 2002), and it was not significantly more luminous than the average SN Ic. Also, SN 2002ap was not seen in association with a GRB (Hurley et al. 2002; Gal-Yam, Ofek, & Shemmer 2002).

Mazzali et al. (2002) modelled the early-time light curve and spectral evolution of SN 2002ap and derived values of the ejected mass ($M_{\text{ej}} = 2.5 - 5 M_\odot$), the kinetic energy of the explosion ($E_{\text{kin}} = 4 - 10 \times 10^{51} \text{ erg}$), and the mass of ^{56}Ni synthesised in the explosion ($M(^{56}\text{Ni}) = 0.07 M_\odot$). While the mass of ^{56}Ni is similar to that of “normal” SNe Ic (Sauer et al. 2006), and much smaller than that of hypernovae linked to GRBs, both M_{ej} and E_{kin} are intermediate between those of normal SNe Ib/c and GRB-SNe. The uncertainty in the values of M_{ej} and E_{kin} follows from assuming either the absence of any He envelope (lower bound) or the presence of a maximal, $2.5 M_\odot$ helium envelope, the presence of which would not affect the light curve significantly but is at the same time not supported by the spectral appearance of SN 2002ap. Interestingly, the light-curve behavior at advanced phases was very similar to that of SN 1998bw (Tomita et al. 2005), suggesting a common nature for the two events.

Mazzali et al. (2002) argued that SN 2002ap was the $\sim 5 M_{\odot}$ carbon-oxygen core of a star of initially $\sim 25 M_{\odot}$ that collapsed to a black hole. On the other hand, no GRB was detected, only weak radio emission was detected from the SN (Berger, Kulkarni, & Chevalier 2002), and the X-ray signal was very weak (Soria, Pian, & Mazzali 2003), suggesting that little or no relativistic ejecta were produced. This may be related to the relatively small mass of the collapsing star, which may have been close to the minimum required to form a black hole. It is therefore interesting to explore further the nature of this object. As in the case of SNe 1998bw and SN 2006aj, this can be done by modelling the nebular spectra.

Foley et al. (2003) published a series of late-time spectra of SN 2002ap, while Kawabata et al. (2002) published a single spectrum. The nebular phase in SN 2002ap started to develop rather early, as in SN 1998bw but unlike other hypernovae such as SN 1997ef (Mazzali et al. 2004). At an age of ~ 4 months, the SN spectra were already fully nebular (Foley et al. 2003). The optical spectra were dominated by very strong [O I] $\lambda\lambda 6300, 6363$ emission, and showed strong Ca II emission lines, similar to SN 1998bw. Unlike the case of SN 1998bw, however, the [Fe II]-dominated blend near 5200 Å is rather weak. This is not surprising, since SN 1998bw is thought to have produced ~ 4 times as much ^{56}Ni as SN 2002ap (Mazzali et al. 2006). Still, the [Fe II] lines in SN 2002ap are sufficiently pronounced that modelling can be meaningfully attempted. One peculiarity of SN 2002ap is the great strength of the Mg I $\lambda\lambda 4571$ line, which may suggest that the envelope of SN 2002ap was more thoroughly stripped than that of SN 1998bw. This would favor the lower bound of the mass and energy estimates of Mazzali et al. (2002), which were obtained assuming the absence of any significant He layer.

2. The Spectral Dataset

In this paper, we model all the spectra published by Foley et al. (2003). Additionally, we present and model three additional late-time spectra. Two of these spectra were obtained with the Subaru telescope. The other spectrum was obtained at the National Astronomical Observatory of China (NAOC, formerly Beijing Astronomical Observatory, BAO).

The Subaru spectra were obtained on 2002 Jun 7.6 (UT dates are used throughout this paper) and Sep 15.6 with FOCAS. For both spectra, the exposure time was 240 s, and grism B300 and Y47 order-cut filters were used. A $0''.8$ wide slit was used for the June spectrum and the resulting spectral resolution ($\lambda/\Delta\lambda$) is ~ 650 . For the September spectrum, a $2''.0$ slit was used, but the spectral resolution is still similar to that of the June spectrum because the seeing size was $0''.7$ – $0''.8$. The flux was calibrated using observations of either Feige 110 or G191B2B obtained on the same night as the target spectra.

The BAO spectrum was obtained on 2002 July 11.8 with the NAOC 2.16 m telescope at Xinlong Observatory (then BAO). The observations were carried out with an OMR (Optomechanics Research, Inc.) spectrograph, using a Tektronix 1024×1024 pixel CCD as the detector. A grating of 300 g mm^{-1} was used, which provided a spectral resolution of $\sim 10 - 11 \text{ \AA}$. The exposure time was $\sim 40 \text{ min}$.

The newly published spectra are shown in Figure 1. The NAOC spectrum is reasonably consistent with the almost contemporaneous Lick spectrum published by Foley et al. (2003), and therefore it was modelled but is not explicitly shown in the Figures in the following sections.

The 11 spectra we used for modelling cover a time span of almost 9 months, from June 2002 through February 2003, corresponding to SN ages of 4–13 months given that the SN exploded on 29 January 2002 (Mazzali et al. 2002). Unfortunately, the wavelength coverage is not uniform. In particular, the Subaru spectra extend over a shorter range (4700–9000 \AA) than the other spectra, missing the important Mg I] line. Models based on the Subaru spectra are therefore somewhat less reliable than those based on the Lick spectra. All spectra were calibrated by using the available photometry (Foley et al. 2003) with the exception of the last three, for which an extrapolation of the light curve was used.

3. Modelling Technique

In order to model the nebular spectra of SN 2002ap, we used our non-local thermodynamic equilibrium (non-LTE) code (Mazzali et al. 2001). The code computes the heating of the gas following the deposition of γ -rays and positrons emitted by the decay of ^{56}Co into ^{56}Fe . Heating is balanced by cooling via nebular line emission. The emission rate in each line is computed solving a non-LTE matrix of level populations (Axelrod 1980). In the original version (Ruiz-Lapuente & Lucy 1992), a homologously expanding nebula of finite extent, uniform density, and uniform composition is assumed, and the emission spectrum is obtained assigning to all lines a parabolic profile, bounded by the velocity of the outer edge of the nebula.

Together with this classical version, a more advanced — although more model-dependent — version has been developed and is used in this work. In this new version, stratification in density and abundance is adopted. The density profile is taken from explosion models, and γ -rays and positrons are emitted at various depths according to the distribution of ^{56}Ni . Their propagation and deposition is followed using a Monte Carlo scheme similar to that discussed by Cappellaro et al. (1997) for their light-curve models. A constant γ -ray opacity

($\kappa_\gamma = 0.027 \text{ cm}^2 \text{ g}^{-1}$) and a constant positron opacity ($\kappa_{e^+} = 7 \text{ cm}^2 \text{ g}^{-1}$) are assumed. The heating and cooling of the gas are then computed in non-LTE in each radial shell, and so is the line emissivity. The line profiles from each shell are assumed to be truncated parabolas, the inner truncation point corresponding to the inner boundary of the shell considered. These truncated parabolas are then summed to produce the emerging spectrum. Line profiles thus depend on the density and abundance distributions. Therefore, this approach constitutes a test of the explosion models which are used to simulate the light curves and the early-time spectra, especially for what concerns the innermost part, which is only visible directly in the nebular phase.

Because the stratified code depends more directly on the adopted explosion model than the one-zone version, it is useful to compare the results of the two approaches. The next two sections deal with both cases in turn.

One important ingredient for the modelling is the assumed distance and reddening to the SN. In the case of SN 2002ap, the distance is highly uncertain, as discussed by Vinko et al. (2004). Sharina, Karachentsev, & Tikhonov (1996), using the brightest blue supergiant stars, obtained a distance modulus of $\mu = 29.32$ mag for M74, and $\mu = 29.50$ mag for the M74 group, confirming previous results by Sohn & Davidge (1996), who preferred to use red supergiants. As Vinko et al. (2004) comment, this value was derived using the Galactic absorption maps of Burstein & Heiles (1982), which give a value of the total absorption in the B band of $A_B = 0.13$ mag. On the other hand, the more recent maps published by Schlegel, Finkbeiner, & Davis (1998) predict a larger absorption, $A_B = 0.301$ mag, leading to a reduced distance, $\mu = 29.15$ mag.

As for the reddening, combining the Galactic extinction of Schlegel, Finkbeiner, & Davis (1998), $E(B-V)_G = 0.075$ mag, with the small reddening within M74 (Takada-Hidai, Aoki, & Zhao 2002, $E(B-V)_H = 0.020$ mag), a total value of $E(B-V) = 0.09$ mag is used.

Clearly, the uncertainty associated with the distance is the largest contribution to the overall uncertainty on the luminosity of SN 2002ap. Therefore, in this paper we have chosen to adopt the same values used in previous modelling and analysis papers (Mazzali et al. 2002; Yoshii et al. 2003, ($\mu = 29.50$ mag, $E(B-V) = 0.09$ mag)) in order to make the results immediately comparable. The effect of adopting a different value for the distance is discussed below.

4. One-Zone Models

The driving parameters for the one-zone fits are the line width, the mass of ^{56}Ni , and the masses of the other elements. Fitting the widths of the complex [Fe II] blend near 5200 Å gives a measure of the distribution of ^{56}Ni , since most Fe is the product of the decay of ^{56}Ni . This blend can be fitted for a nebular velocity of between 6200 and 5200 km s $^{-1}$. The line width slowly decreases over the period considered, which is in good agreement with what was found for SN 1998bw (Mazzali et al. 2001), although in that case the velocities were significantly larger. This behavior indicates that the outer parts of the ejecta are becoming progressively more difficult to excite as the density decreases owing to the expansion. Unlike the case of SN 1998bw, however, the velocity that is required to fit the [Fe II] lines is also appropriate for the [O I] line. This is typical of lower-energy SNe Ic (e.g., SN 1994I, Sauer et al. 2006), and indicates that the degree of asphericity of the explosion is small. The only apparent deviation from sphericity is the presence of narrow emission spikes in the cores of [O I] $\lambda\lambda 6300, 6363$ and Mg I] $\lambda 4571$, at velocities below 2000 km s $^{-1}$ (Foley et al. 2003, Figure 17). Such a feature was also observed in SN 2006aj (Mazzali et al. 2007).

The masses of the other elements are determined by fitting the various emission lines. One caveat is that two intermediate-mass elements that are expected to be abundant in the SN ejecta are only diagnosed by a single line. The only line of sulfur is [S I] $\lambda\lambda 4069$, which is blended with various Fe lines. Silicon, a highly abundant element, also has no strong or isolated line at optical wavelengths. A shoulder on the red side of [O I] $\lambda\lambda 6300, 6363$ may be due to [Si I] $\lambda 6527$. We have determined the masses of Si and S by trying to reproduce those two features, but the uncertainty involved is large, affecting also the estimate of the mass in the ejecta. In fact, both silicon and sulfur have strong lines in the infrared ([Si I] 1.61, 1.65 μm , [S I] 1.08, 1.13 μm), which act as efficient coolants. Thus, increasing the mass of these two elements requires all other masses, including that of ^{56}Ni , to be increased. Additionally, since in the later spectra it is not possible to reproduce accurately the red shoulder of the [O I] line, there may be some doubt as to the actual contribution of silicon to that feature. More accurate statements about the masses of these elements would require the availability of infrared spectra.

As in SN 1998bw, the spectra of SN 2002ap show lines of [Fe II], but not [Fe III]. This implies a rather low degree of ionization, which can be reproduced assuming significant clumping to favor recombination. As in Mazzali et al. (2001), a volume filling factor of 0.1 was adopted in all models to achieve this. The models with stratified density and composition discussed in the next section are useful to address this issue.

The results are summarized in Table 2, and the time series of the spectral fits is shown in Figures 1 and 2. The electron temperature and density in the nebula decrease with

time. The inferred value of $M(^{56}\text{Ni})$ is $\sim 0.10 M_{\odot}$. Small oscillations around this value in the various fits are probably due to a combination of inconsistent flux calibration and incomplete wavelength coverage, in particular for spectra that do not include the Mg I] line. Only in the two very late-time spectra does the ^{56}Ni mass increase significantly, but these spectra are calibrated in flux using an extrapolation of the observed photometry, making the results less reliable.

In order to fit the spectra, we require an ejected mass of $\sim 1.6 - 1.9 M_{\odot}$ below a velocity of 5500 km s^{-1} . Of this mass, $\sim 0.7 M_{\odot}$ is oxygen. The density profile (CO100/4) used by Mazzali et al. (2002) to fit the early-time light curve and spectra only contained $\sim 0.8 M_{\odot}$ below the same velocity. Interestingly, the larger mass is in good agreement with the results of Maeda et al. (2003), who used a two-component, one-dimensional density distribution to reproduce the light curve of SN 2002ap and obtained a ^{56}Ni mass of $0.08 M_{\odot}$ and an ejected mass of $1.6 M_{\odot}$ below 5750 km s^{-1} (see also Tomita et al. 2005). Although the mass at low velocity may be somewhat overestimated by the one-zone models, which overfit the flux at the lowest velocities where the observed [O I] line has a narrow core, the need for additional mass at low velocity is clear. Similar results were also obtained for other SNe Ic (e.g., Sauer et al. 2006; Mazzali et al. 2007). They suggest the presence of a dense, oxygen-rich core in the ejecta, which would be most naturally explained as the result of an aspherical explosion.

One place where our models fail is the emission near 7700 \AA . This is likely to be O I $\lambda 7774$. The excitation temperature of this line is significantly higher than the nebular temperatures obtained in our models, suggesting that the flux in the line may be caused by recombination or non-thermal excitation by fast electrons.

Therefore, while the results from the one-zone models generally confirm findings from the light curve and spectral study of Mazzali et al. (2002), they suggest that the improvements introduced by Maeda et al. (2003) are realistic, and that a simple one-dimensional explosion model is not sufficient to explain the behavior of SN 2002ap.

5. Multi-Zone Models

We have modelled the same 11 spectra of SN 2002ap with the multi-zone code described in Section 2. As a model of the explosion, we selected CO100/4, which was used by Mazzali et al. (2002) to fit the early-time light curve and spectra of SN 2002ap.

Our multi-zone code is still one-dimensional, but by allowing us to investigate the element distribution in velocity space at an epoch when the ejecta are fully transparent, it

can give us indirect clues of possible asymmetries through unusual abundance distributions. Therefore, although we started our models using the density profile and the abundances of CO100/4, we allowed the abundances to vary so as to achieve the best possible fit to the data. Repeating this exercise over several epochs ensures the validity of the results.

Also, because the ejecta are assumed to be fully transparent, once the abundance distribution has been defined from fitting one spectrum, it should not need to be changed to reproduce the other epochs. Ideally, this should be done with the earliest nebular spectrum, since this is likely to show emission from a broader range of velocities than later spectra, as discussed in the previous section.

Since the first spectrum of our series does not cover the Mg I] $\lambda 4571$ line, which is an important coolant, we used as reference the Lick Observatory 8 June 2002 spectrum, which offers very broad wavelength coverage at a high signal-to-noise ratio. The model used to fit that spectrum gave good results for the other spectra, with only small changes in composition, which may be attributed to the variable observing conditions and flux calibration.

The series of our synthetic spectra is shown in Figures 4 and 5. In order to reproduce the width of the [Fe II] lines, the mass fraction of ^{56}Ni must be small ($\sim 1\%$) at $9000 < v < 17,000 \text{ km s}^{-1}$, and then slowly increase inward, reaching $\sim 10\%$ at $3000 < v < 6000 \text{ km s}^{-1}$. At the lowest velocities, below 3000 km s^{-1} , the abundance drops again to $\sim 2\%$. For the highest velocities ($v > 17,000 \text{ km s}^{-1}$), the value of the abundance derived from the early-time modelling ($\sim 10\%$) was used, but this does not affect the nebular spectra. The oxygen mass fraction, on the other hand, does not change significantly with velocity. It is $\sim 65\%$ at $v > 10,000 \text{ km s}^{-1}$, decreasing to $\sim 40\%$ at $2000 < v < 7000 \text{ km s}^{-1}$, a region that is dominated by ^{56}Ni , Si, and S. The abundance of S was determined from the weak [S I] $\lambda 4069$ line, and the Si abundance was assumed to have a constant ratio of 3:1 with respect to that of S. With this assumption, the emission on the red side of the [O I] line is not fully reproduced, suggesting that [Si II] is not the only line contributing to it, or that a larger mass, or a larger Si/S ratio should be adopted. Other elements behave as expected. The Mg and Ca abundances also increase inward, while C decreases with O.

One problem using model CO100/4 is that the strong, narrow cores of [O I] $\lambda\lambda 6300, 6363$ and Mg I] $\lambda 4571$ cannot be reproduced. The characteristic velocities of these cores are in fact $< 2000 \text{ km s}^{-1}$, but CO100/4 has a density “hole” at $v < 3000 \text{ km s}^{-1}$. Therefore, following Maeda et al. (2003), we added a dense inner region at $v < 3000 \text{ km s}^{-1}$. The composition of this region must be dominated by O, with C, Mg, and other intermediate-mass elements also present so that the line cores can be reproduced. However, only little ^{56}Fe must be present there, or the [Fe II] feature would be negatively affected. This inner zone contains only $\sim 0.2 M_{\odot}$ of material, mostly oxygen. The total ^{56}Ni mass below 3000 km s^{-1} is $\sim 0.01 M_{\odot}$,

in agreement with the result of Maeda et al. (2003). The oxygen mass below 5750 km s^{-1} in these models is $0.35 M_{\odot}$, which is significantly less than in the one-zone models. The total ^{56}Ni mass is, however, slightly larger ($\sim 0.11 M_{\odot}$). The total ejected mass is $M_{\text{ej}} \approx 2.5 M_{\odot}$, of which $\sim 1.3 M_{\odot}$ is oxygen.

The main results obtained from the multi-zone models are recapped in Table 2. The last two spectra again require a somewhat larger ^{56}Ni mass. Because of the uncertain flux calibration of these spectra, we do not regard this as an inconsistency of our modelling procedure. The oxygen mass is, however, much more stable than in the one-zone models, showing that the multi-zone approach is more accurate, and that the explosion model that we used is a good representation of the ejecta of SN 2002ap in the late phase as well as the early phase.

One further point concerns clumping. Introducing a density gradient should reduce the ionization degree at low velocity. Thus, it may be expected that in the stratified models clumping would not be necessary. However, even in these models, if clumping is not used the Fe ionization is too high at all velocities. A filling factor of 0.1 was therefore used in all zones with $v > 2000 \text{ km s}^{-1}$ — that is, wherever ^{56}Ni is present. No clumping is necessary in the O-dominated inner zone, below 2000 km s^{-1} . There are a number of possible explanations for this. One is that clumping does indeed exist. The lack of direct evidence (e.g., narrow emission features at different velocities) suggests that any clumps must be small and evenly distributed in velocity space. Another possibility is that ^{56}Ni is located mostly near the jet direction in an axisymmetric explosion. In this case, the actual density of Fe in the effectively emitting volume in the nebular phase would be higher than what is suggested by a spherically symmetric approach like the one used here. Clumping would then be a proxy for this aspherical distribution. The total mass estimate would not be affected, since in the nebular phase each emitting ion contributes to the line profile, independent of its position. An axisymmetric configuration was indeed suggested for the outer part of the ejecta as a possible interpretation of the detection of significant line polarization in the early-time spectra of SN 2002ap (Kawabata et al. 2002; Leonard et al. 2002). If significant asymmetry affected the inner part of the ejecta, the profiles of the nebular emission lines would depend sensitively on viewing angle, as demonstrated by Maeda et al. (2002) for SN 1998bw. However, in this case the lack of a coincident GRB and of dramatic signatures of asphericity in the nebular spectra suggest that any deep asphericity was most likely weak.

6. The Geometry of the Ejecta of SN 2002ap

We have modelled a series of nebular spectra of the broad-lined SN 2002ap, using a one-zone non-LTE code and a multi-zone code where γ -ray deposition and line emission are computed more accurately based on a pre-defined explosion model. Both simulations yield a good reproduction of the [Fe II] lines, but the narrow cores observed in [O I] $\lambda\lambda 6300, 6363$ can only be reproduced assuming the presence of a dense, O-dominated inner zone. In the one-zone synthetic spectra, a mass excess of $\sim 0.7 M_\odot$ is needed to reproduce qualitatively the [O I] emission line. In the multi-zone model, which reproduces the line profiles much more accurately, the mass excess is smaller, $\sim 0.2 M_\odot$, but the presence of oxygen-dominated material moving at low velocity is confirmed. This material is not predicted by one-dimensional explosion models, but its presence was suggested in various hypernovae based on light-curve studies (Maeda et al. 2003).

Similar results were also obtained for the normal SN Ic 1994I (Sauer et al. 2006) as well as for the XRF/SN 2006aj (Mazzali et al. 2007). SN 1994I shows emission in the [O I] $\lambda\lambda 6300, 6363$ line at velocities below 2000 km s^{-1} (Filippenko et al. 1995), while the corresponding one-dimensional explosion model predicts the absence of material at low velocities. The rounded profile suggests a smooth distribution of oxygen, which does not by itself indicate an aspherical explosion, but the very presence of material does, and it can be modelled adding $0.2 M_\odot$ of oxygen-dominated mass at low velocity. SN 2006aj shows a peak in [O I] $\lambda\lambda 6300, 6363$ at velocities below 2000 km s^{-1} , although not quite as sharp as in SN 2002ap (Figure 4). This was modelled for a mass excess of $\sim 0.7 M_\odot$ over the one-dimensional explosion model (Mazzali et al. 2007). The presence of a dense inner zone in all SNe Ic suggests that these explosions are intrinsically aspherical, as is also deduced from polarization studies (Wang et al. 2001; Leonard et al. 2002; Filippenko & Leonard 2004; Leonard & Filippenko 2005).

Figure 6 shows a comparison of the [O I] $\lambda\lambda 6300, 6363$ line in SN 2002ap, and in SNe 2006aj, 1998bw, and 2003jd (Mazzali et al. 2007, 2001, and 2005, respectively). The line in SN 2006aj has a full-width at half-maximum intensity (FWHM) of $\sim 8000 \text{ km s}^{-1}$, while for the other three SNe the FWHM is $\sim 6000 \text{ km s}^{-1}$. The line profile in SN 2006aj is not very sharp, indicating that the nebula is to a good approximation spherically symmetric (Mazzali et al. 2007). In this case the [O I] line velocity should correspond to the real expansion velocity. The sharp profile in SN 1998bw was interpreted as a disk-like distribution of oxygen viewed from a near-polar direction. Although the low observed velocity is partly the result of a projection effect, the actual velocity of the oxygen ($\sim 8000 \text{ km s}^{-1}$) is smaller than the velocity of Fe (Maeda et al. 2002). The [O I] line of SN 2003jd has a width similar to that of SN 1998bw, but the double-peaked profile suggests that we are viewing

the oxygen-rich disk from near its plane (Mazzali et al. 2005). The case of SN 2002ap seems intermediate between those of SNe 1998bw and 2006aj. The line can be separated into two components. A broad base, of width similar to that in SNe 1998bw and 2003jd, is present down to velocities of $\sim 3000 \text{ km s}^{-1}$ and is well fitted by a one-zone model. Its profile is reminiscent of that of SN 2003jd, but the presence of the sharp core makes it impossible to distinguish between a flat-topped profile, characteristic of a shell-like spherical distribution, and a double-peaked profile as in a disk viewed edge-on. This core is narrower than even the corresponding profile of SN 1998bw.

There may be two explanations for this type of profile. One is that in SN 2002ap the outer part of the oxygen, from $v \approx 3000$ out to $v \approx 8000 \text{ km s}^{-1}$, has a distribution that is not far from spherical, giving rise to a flat-topped profile. Below $\sim 3000 \text{ km s}^{-1}$, on the other hand, we may be seeing a situation qualitatively similar to that of SN 1998bw, with the oxygen distributed in a disk-like region oriented not far from face-on. The size and mass of this disk-like region are, however, much smaller in SN 2002ap than in SN 1998bw. The other possibility is that the outer part reflects a disk-like distribution of most of the oxygen viewed not far from its plane, like in SN 2003jd. The broad component of the profile would then be double-peaked rather than flat-topped, and the inner component would contain more mass, so that its emission could fill the valley between the two peaks. The sharpness of this inner-component emission may again indicate a disk-like distribution viewed face-on, but in this case two main orientations would exist in the ejecta, which may not be easy to explain in terms of the collapse mechanism. Alternatively, the inner region could simply be sharply peaked in density, as reproduced by our multi-zone model, but not grossly aspherical.

In both scenarios the lack of a GRB may be justified. If the inner explosion was aspherical, but the asphericity did not propagate to the intermediate part of the ejecta (3000 to 8000 km s^{-1}), it is unlikely that a beam of material moving at relativistic velocities was produced, yet the overenergetic explosion could have caused enough material to move at high velocities ($\sim 30000 \text{ km s}^{-1}$), giving rise to the broad absorption features in the early spectra. The distribution of this material may not have been very far from spherical: polarization studies (Kawabata et al. 2002; Leonard et al. 2002) suggest a degree of asphericity of $\sim 10\%$. On the other hand, if the outer explosion was aspherical, a relativistic jet may have been produced, but it would not have been pointing to us. This latter possibility is, however, not supported by the lack of an X-ray detection (Soria, Pian, & Mazzali 2003) and the weakness of the radio signal (Berger, Kulkarni, & Chevalier 2002), so we tend to favor an explosion that was not far from spherical, except in the innermost part.

Both simulations agree that the ^{56}Ni mass ejected by SN 2002ap is $\sim 0.10 M_{\odot}$, a slightly larger value than that predicted by studies of the early-time light curve (Mazzali et al. 2002),

but in agreement with the late-time light curve (Maeda et al. 2003; Tomita et al. 2005). The multi-zone model confirms that only a small fraction of this ($\sim 0.01 M_{\odot}$) is located in the innermost zone, a clear indication that the explosion was asymmetric to some degree.

Other global values that can be derived rather accurately from a one-dimensional study of the nebular spectra ($M(^{56}\text{Ni}) \approx 0.11 M_{\odot}$, $M_{\text{ej}} \approx 2.5 M_{\odot}$) are small compared to those of other broad-lined SNe, confirming previous results based on the early-time light curve and spectra. These values point to a progenitor less massive than for objects such as SN 1998bw or SN 2003dh, although still a massive star ($M \approx 22 - 25 M_{\odot}$) that could have produced a black hole. This also suggests that the “hypernova” properties of SN 2002ap were less extreme, including asymmetry and the launching of a GRB.

The estimated mass of ^{56}Ni would be smaller if we adopted a shorter distance. If the distance modulus was $\mu = 29.15$ mag, the ^{56}Ni mass would be reduced by $\sim 15\%$. The mass and energy of the ejecta would also be similarly reduced, but the change is sufficiently small that the shape of the light curve would not be affected.

Indirect indications of asymmetry can be obtained in our one-dimensional study, but the details of the exact properties are not. The development of axisymmetric explosion models suitable for SN 2002ap, and the study of the nebular spectra using three-dimensional spectrum synthesis codes as in Maeda et al. (2002), are currently planned.

The work of A.V.F.’s group at UC Berkeley is supported by National Science Foundation grant AST-0607485. We thank the Subaru and Lick Observatory staffs for their assistance with the observations.

REFERENCES

Axelrod, T. S. 1980, Ph.D. thesis, Univ. of California, Santa Cruz

Berger, E., Kulkarni, S. R., & Chevalier, R. A., 2002, ApJ, 577, L5

Burstein, D., & Heiles, C., 1982, AJ, 87, 1165

Cappellaro, E., Mazzali, P. A., Benetti, S., Danziger, I. J., Turatto, M., Della Valle, M., & Patat, F. 1997, A&A, 328, 203

Deng, J., Tominaga, N., Mazzali, P. A., Maeda, K., & Nomoto, K. 2004, ApJ, 624, 898

Duncan, R. C., & Thompson, C. 1992, ApJ, 392, L9

Filippenko, A. V. 1997, *ARA&A*, 35, 309

Filippenko, A. V., & Leonard, D. C. 2004, in *Cosmic Explosions in Three Dimensions*, ed. P. Höflich, P. Kumar, & J. C. Wheeler (Cambridge: Cambridge Univ. Press), 30

Filippenko, A. V., et al. 1995, *ApJ*, 450, L11

Foley, R. J., et al. 2003, *PASP*, 115, 1220

Fynbo, J. P. U., et al. 2003, *ApJ*, 609, 962

Galama, T. J., et al. 1998, *Nature*, 395, 670

Gal-Yam, A., Ofek, E. O., & Shemmer, O. 2002, *MNRAS*, 332, L73

Hurley, K., et al. 2002, *GCN Circ.* 1252

Heise, J., in't Zand, J., Kippen, R. M., & Woods, P. M. 2001, in *Gamma-ray Bursts in the Afterglow Era*, ed. E. Costa, F. Frontera, & J. Hjorth (Berlin: Springer), 16

Iwamoto, K., et al. 1998, *Nature*, 395, 672

Kawabata, K., et al. 2002, *ApJ*, 580, L39

Kinugasa, K., et al. 2002, *ApJ*, 577, L97

Leonard, D. C., & Filippenko, A. V. 2005, in *1604–2004, Supernovae as Cosmological Light-houses*, ed. M. Turatto, et al. (San Francisco: ASP), 330

Leonard, D. C., Filippenko, A. V., Chornock, R., & Foley, R. J. 2002, *PASP*, 1333, 1348

MacFadyen, A. I., & Woosley, S. E. 1999, *ApJ*, 524, 262

Maeda, K., Nakamura, T., Nomoto, K., Mazzali, P. A., Patat, F., & Hachisu, I., *ApJ*, 565, 405

Maeda, K., et al. 2003, *ApJ*, 593, 931

Maeda, K., Mazzali, P. A., & Nomoto, K., *ApJ*, 645, 1331

Maeda, K., et al. 2007, *ApJ*, 658, L5

Malesani, D., et al. 2004, *ApJ*, 609, L5

Mazzali, P. A., Deng, J., Maeda, K., Nomoto, K., Filippenko, A. V., & Matheson, T. 2004, *ApJ*, 614, 858

Mazzali, P. A., Nomoto, K., Patat, F., & Maeda, K., et al. 2001, 559, 1047

Mazzali, P. A., et al. 2002, ApJ, 572, L61

Mazzali, P. A., et al. 2003, ApJ, 599, L95

Mazzali, P. A., et al. 2005, Science, 308, 1284

Mazzali, P. A., et al. 2006a, ApJ, 645, 1323

Mazzali, P. A., et al. 2006b, Nature, 442, 1018

Mazzali, P. A., et al. 2007, ApJ, in press

Modjaz, M., et al. 2006, ApJ, 645, L21

Nakamura, T., Mazzali, P. A., Nomoto, K., & Iwamoto, K. 2001, ApJ, 550, 991

Nomoto, K., Maeda, K., Tominaga, N., Ohkubo, T., Deng, J., & Mazzali, P. A. 2005, Ap&SS, 298, 81

Patat, F., et al. 2001, ApJ, 555, 900

Pian, E., et al. 2006, Nature, 442, 1011

Ruiz-Lapuente, P., & Lucy, L. B. 1992, ApJ, 400, 127

Sauer, D., et al. 2006, MNRAS, 369, 1939

Schlegel, D., Finkbeiner, D., & Davis, M., 1998, ApJ500, 525

Sharina, M. E., Karachentsev, I. D., & Tikhonov, N. A. 1996, A&AS, 119, 499

Soderberg, A. M., et al. 2006, Nature, 442, 1014

Sohn, Y.-J., & Davidge, T.J., 1996, AJ, 111, 2280

Soria, R., Pian, E., & Mazzali, P. A., 2003, A&AS, 413, 107

Stanek, K. Z., et al. 2003, ApJ, 591, L17

Takada-Hidai, M., Aoki, W., & Zhao, G. 2002, PASJ, 54, 899

Thompson, T. A., Chang, P., & Quataert, E. 2004, ApJ, 611, 380

Tominaga, N., Deng, J., Mazzali, P. A., Maeda, K., Nomoto, K., Pian, E., Hjorth, J., & Fynbo, J. P. U. 2003, ApJ, 612, L105

Tomita, H., et al. 2005, ApJ, 644, 400

Vinko, J., et al. 2004, A&AS, 427, 453

Wang, L., Howell, D. A., Höflich, P., & Wheeler, J. C., 2001, ApJ, 550, 1030

Woosley, S. E., & Bloom, J. S. 2006, ARA&A, 44, 507

Yoshii, Y., et al. 2003, ApJ, 592, 467

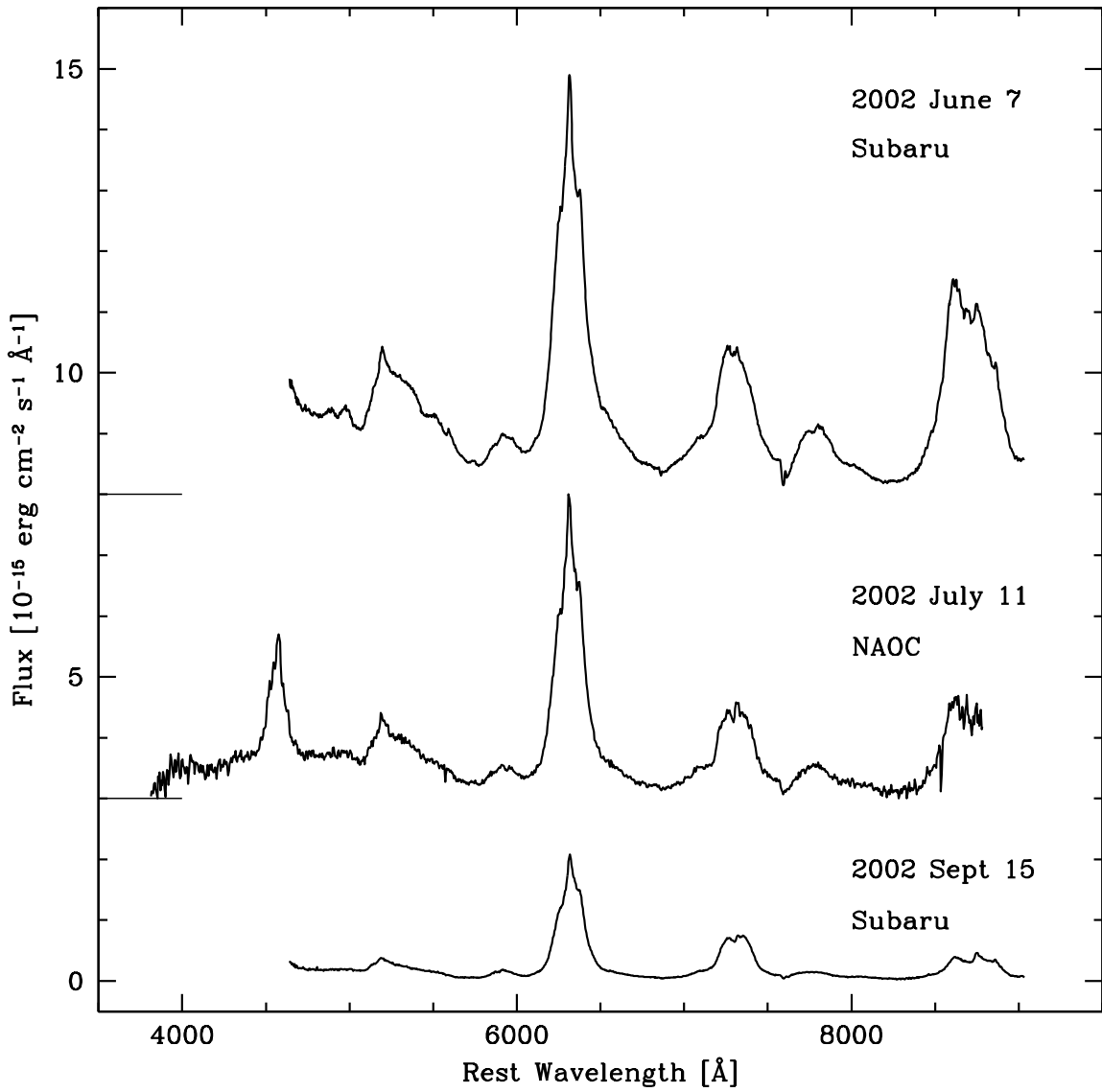


Fig. 1.— The nebular spectra of SN 2002ap obtained at Subaru and NAOC. The two earlier spectra have been shifted upward by adding a constant. The zero level of the flux is shown by a thin horizontal line.

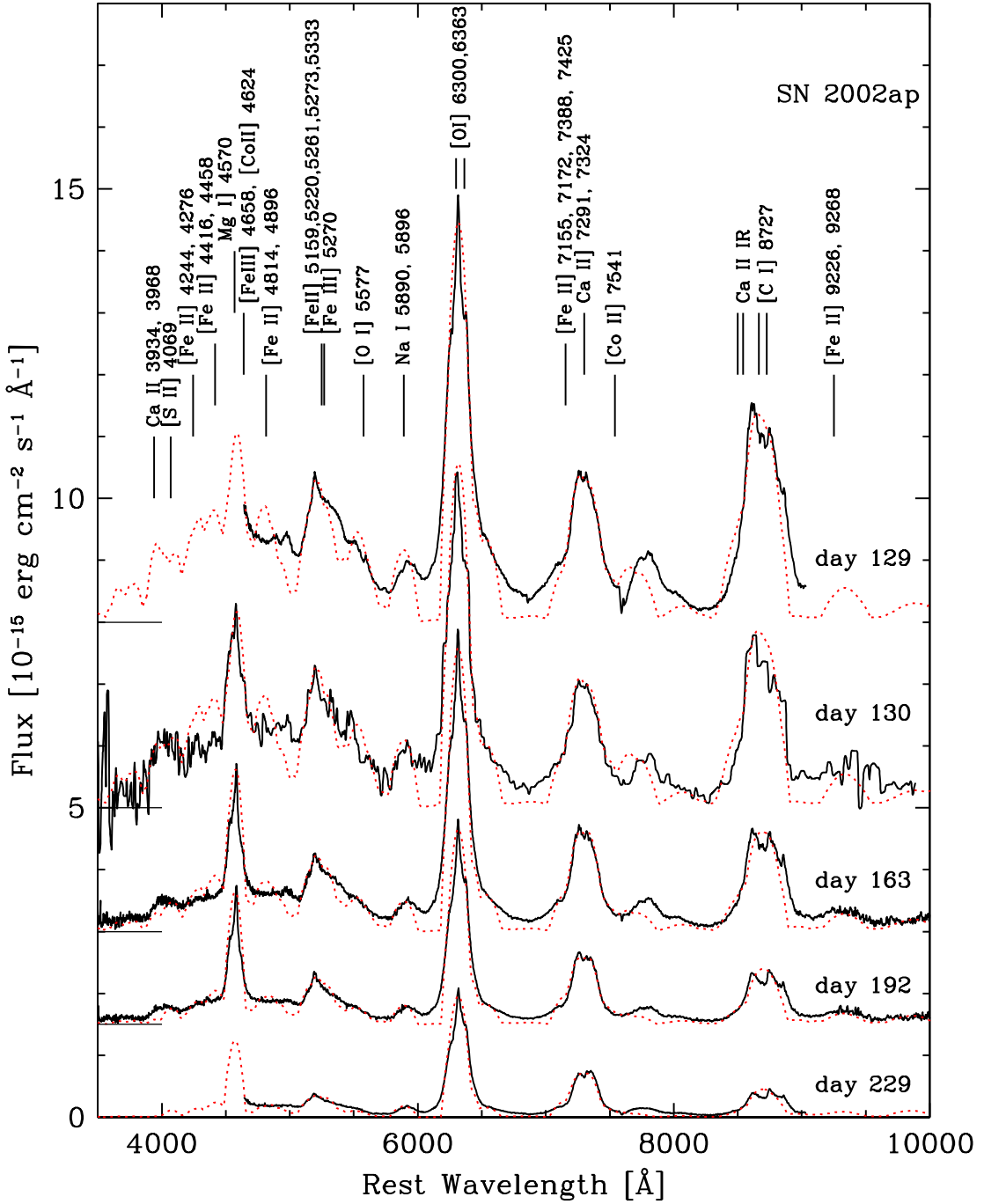


Fig. 2.— The nebular spectra of SN 2002ap obtained from 2002 June to 2002 September, compared to the synthetic spectra computed with the one-zone model (dotted/red). Except for the lowest one, all spectra have been shifted upward by arbitrary amounts. Long tick marks on the left ordinate axis show the zero flux level for each spectrum. [See the electronic edition for a color version of this figure.]

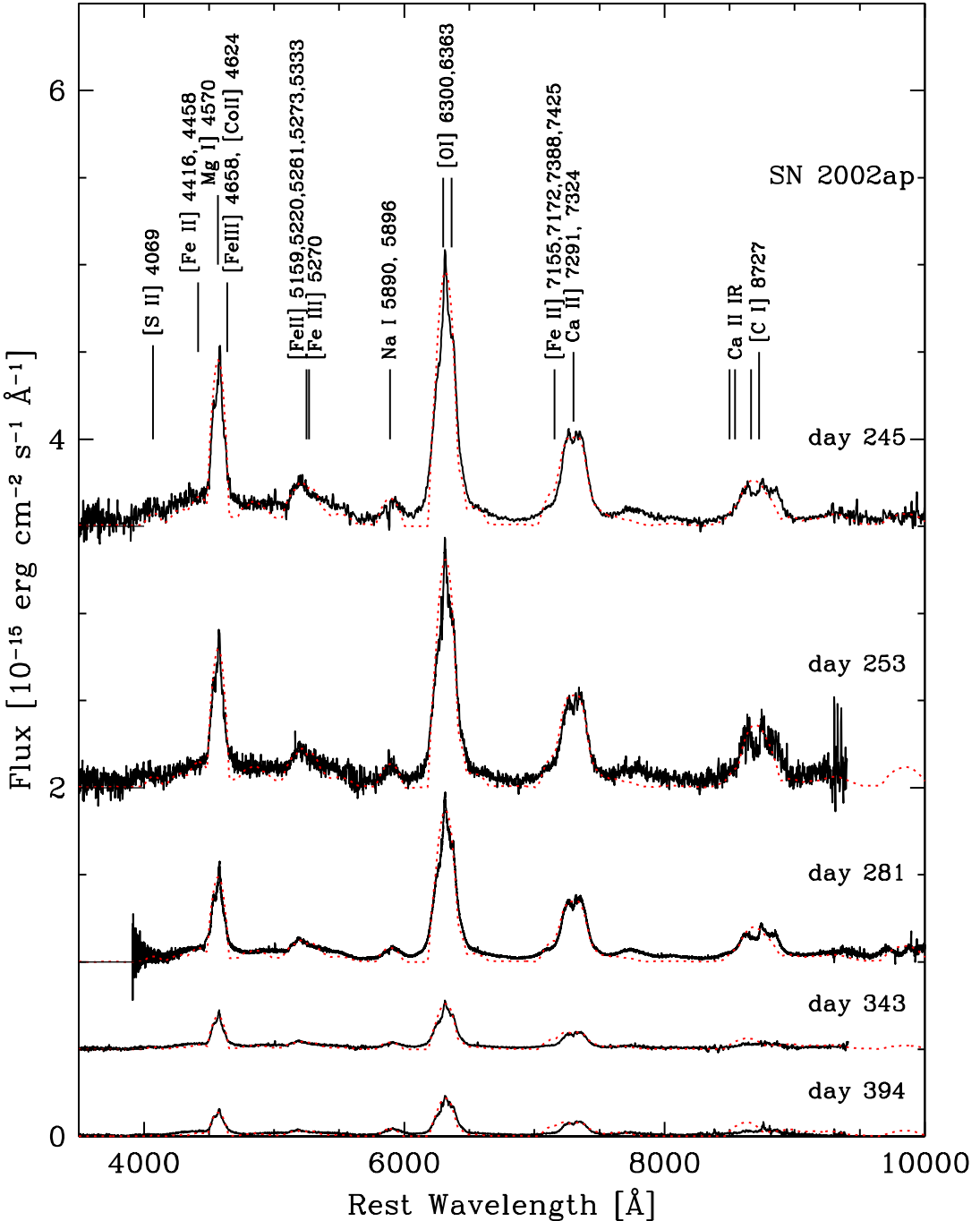


Fig. 3.— The nebular spectra of SN 2002ap obtained from 2002 October to 2003 February, compared to the synthetic spectra computed with the one-zone model (dotted/red). Except for the lowest one, all spectra have been shifted upward by arbitrary amounts. Both the lowest spectrum and the corresponding model have been multiplied by a factor of 2 for display purposes. Long tick marks on the left ordinate axis show the zero flux level for each spectrum. [See the electronic edition for a color version of this figure.]

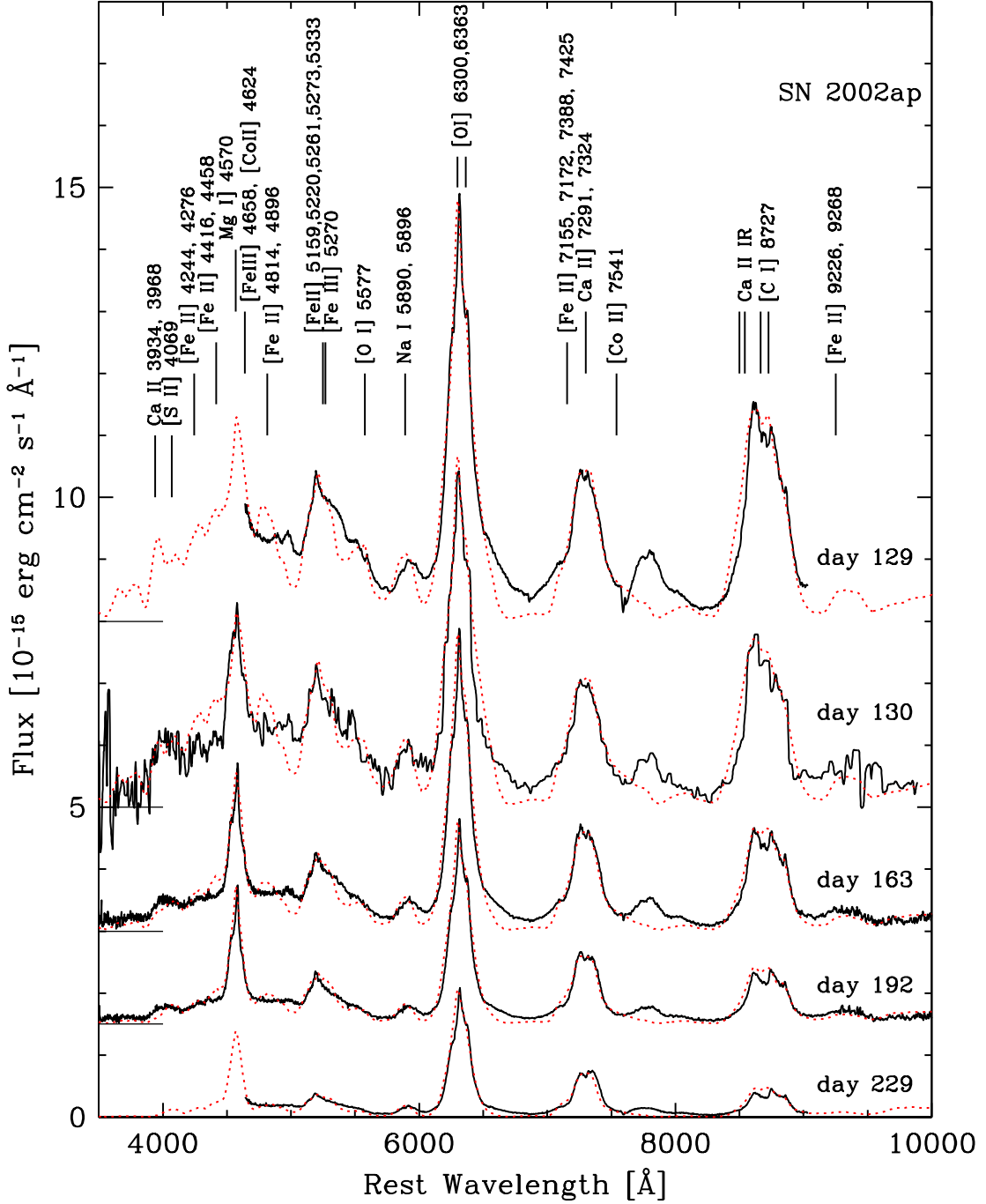


Fig. 4.— The nebular spectra of SN 2002ap obtained from 2002 June to 2002 September, compared to the synthetic spectra obtained with the multi-shell model (dotted/red). Except for the lowest one, all spectra have been shifted upward by arbitrary amounts. Long tick marks on the left ordinate axis show the zero flux level for each spectrum. [See the electronic edition for a color version of this figure.]

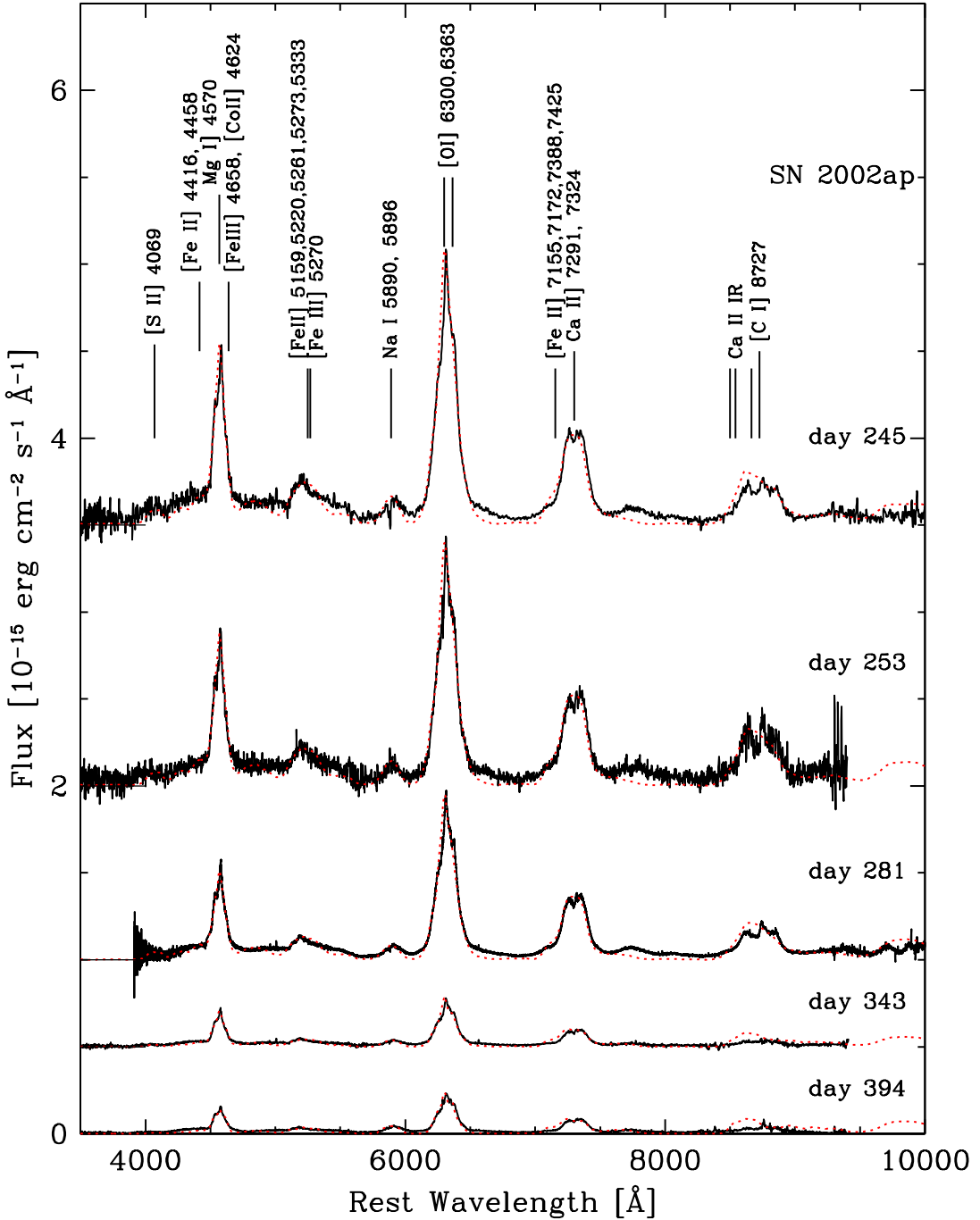


Fig. 5.— The nebular spectra of SN 2002ap obtained from 2002 October to 2003 February, compared to the synthetic spectra computed with the multi-shell model (dotted/red). Except for the lowest one, all spectra have been shifted upward by arbitrary amounts. Both the lowest spectrum and the corresponding model have been multiplied by a factor of 2 for display purposes. Long tick marks on the left ordinate axis show the zero flux level for each spectrum. [See the electronic edition for a color version of this figure.]

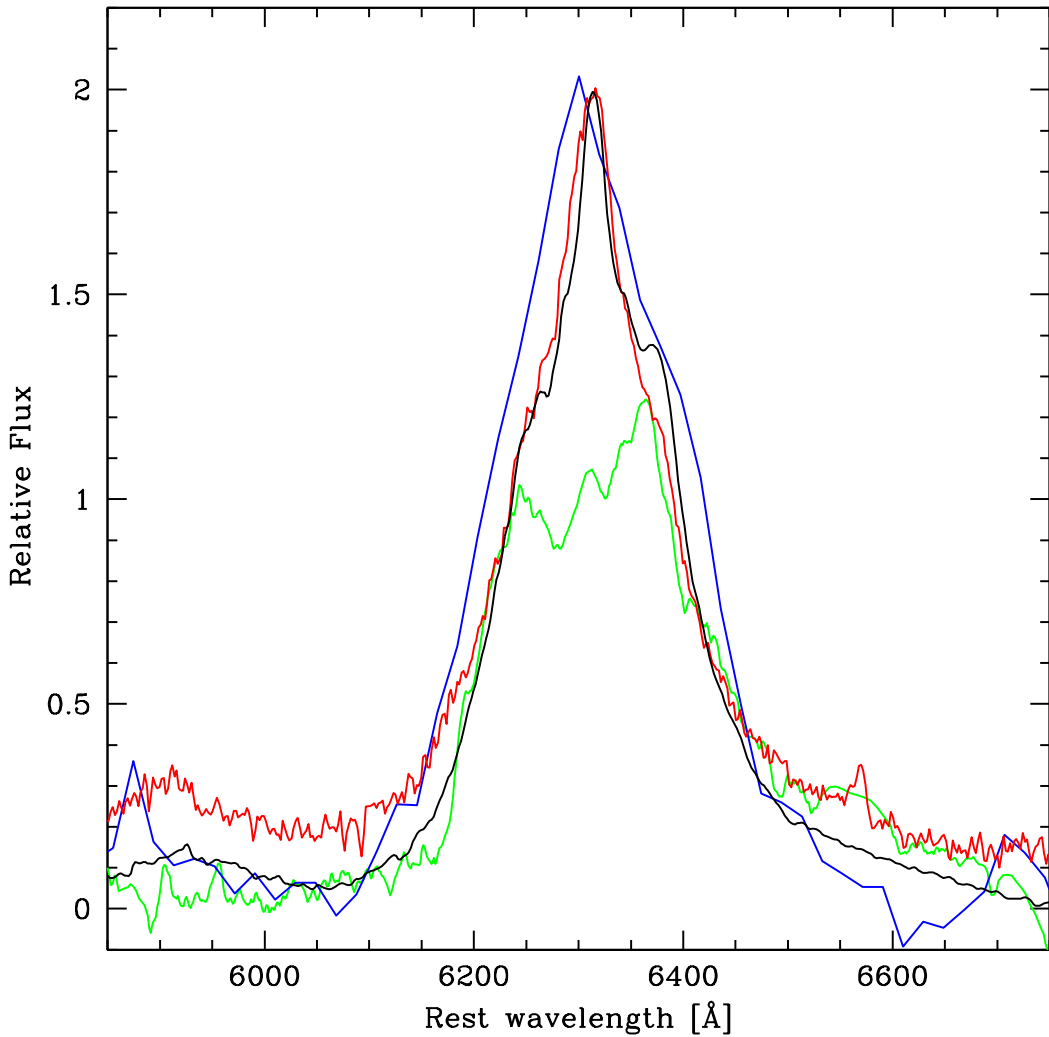


Fig. 6.— A comparison of the [O I] $\lambda\lambda 6300, 6363$ line of SNe 2002ap (solid grey/black line), 2006aj (long dashed/blue line), 1998bw (dotted/red line, Patat et al. 2001), and 2003jd (short dashed/green line, Mazzali et al. 2005). Spectra have been scaled by various amounts to facilitate comparison. [See the electronic edition for a color version of this figure.]

Table 1. Parameters of the One-Zone Synthetic Spectra

UT Date	SN epoch [days] ^a	Telescope	velocity [km s ⁻¹]	$M(^{56}\text{Ni})$ [M_{\odot}]	$M(\text{O})$ [M_{\odot}]	$M(\text{Si})$ [M_{\odot}]	$M(\text{tot})$ [M_{\odot}]	T_e [K]	$\log (n_e /$ (g cm ⁻³))
7 June 2002	129	Subaru	6200	0.090	0.71	0.60	1.78	5511	7.58
8 June 2002	130	Lick 3 m	6200	0.092	0.62	0.50	1.58	5488	7.56
11 July 2002	163	Lick 3 m	5750	0.088	0.71	0.57	1.73	5051	7.34
11 July 2002	163	NAOC	5750	0.090	0.71	0.58	1.73	5082	7.35
9 Aug 2002	192	Lick 3 m	5550	0.093	0.66	0.60	1.69	4751	7.17
15 Sept 2002	229	Subaru	5550	0.098	0.70	0.74	1.90	4360	6.95
1 Oct 2002	245	Lick 3 m	5550	0.102	0.67	0.78	1.86	4209	6.86
8 Oct 2002	253	Lick 3 m	5550	0.103	0.66	0.70	1.88	4160	6.82
6 Nov 2002	281	Lick 3 m	5550	0.110	0.71	0.80	2.04	3903	6.69
7 Jan 2003	343	Lick 3 m	5450	0.145	0.61	0.80	1.93	3422	6.49
27 Feb 2003	394	Lick 3 m	5200	0.170	0.62	0.80	1.92	3092	6.37

^aThe epoch is given from the putative date of explosion, 29 Jan 2002 (Mazzali et al. 2002).

Table 2. Parameters of the Multi-Zone Synthetic Spectra

UT Date	SN epoch [days] ^a	Telescope	$M(^{56}\text{Ni})$ [M_{\odot}]	$M(\text{O})$ [M_{\odot}]	$M(\text{Si})$ [M_{\odot}]
7 June 2002	129	Subaru	0.11	1.21	0.44
8 June 2002	130	Lick 3 m	0.11	1.13	0.58
11 July 2002	163	Lick 3 m	0.11	1.33	0.31
11 July 2002	163	NAOC	0.11	1.33	0.31
9 Aug 2002	192	Lick 3 m	0.12	1.28	0.36
15 Sept 2002	229	Subaru	0.11	1.34	0.29
1 Oct 2002	245	Lick 3 m	0.11	1.29	0.36
8 Oct 2002	253	Lick 3 m	0.11	1.29	0.33
6 Nov 2002	281	Lick 3 m	0.11	1.29	0.31
7 Jan 2003	343	Lick 3 m	0.13	1.28	0.36
27 Feb 2003	394	Lick 3 m	0.13	1.35	0.30

^aThe epoch is given from the putative date of explosion, 29 Jan 2002 (Mazzali et al. 2002).